
Long-Term Variability of the Wind Field over the Indian Ocean Based on ERA-Interim Reanalysis

R. Rashmi¹, V. Polnikov², F. Pogarskii², I. Gomorev², V. Samiksha¹ and P. Vethamony^{1,*}

¹CSIR-National Institute of Oceanography, Dona Paula, Goa, India

²Obukhov Institute of Atmospheric Physics of RAS, Moscow, Russia

[Original manuscript received 15 May 2015; accepted 6 January 2016]

ABSTRACT A detailed study of long-term variability of winds using 30 years of data from the European Centre for Medium-range Weather Forecasts global reanalysis (ERA-Interim) over the Indian Ocean has been carried out by partitioning the Indian Ocean into six zones based on local wind extrema. The trend of mean annual wind speed averaged over each zone shows a significant increase in the equatorial region, the Southern Ocean, and the southern part of the trade winds. This indicates that the Southern Ocean winds and the southeast trade winds are becoming stronger. However, the trend for the Bay of Bengal is negative, which might be caused by a weakening of the monsoon winds and northeast trade winds. Maximum interannual variability occurs in the Arabian Sea due to monsoon activity; a minimum is observed in the subtropical region because of the divergence of winds. Wind speed variations in all zones are weakly correlated with the Dipole Mode Index (DMI). However, the equatorial Indian Ocean, the southern part of the trade winds, and subtropical zones show a relatively strong positive correlation with the Southern Oscillation Index (SOI), indicating that the SOI has a zonal influence on wind speed in the Indian Ocean. Monsoon winds have a decreasing trend in the northern Indian Ocean, indicating monsoon weakening, and an increasing trend in the equatorial region because of enhancement of the westerlies. The negative trend observed during the non-monsoon period could be a result of weakening of the northeast trade winds over the past few decades. The mean flux of kinetic energy of wind (FKEW) reaches a minimum of about 100 W m^{-2} in the equatorial region and a maximum of about 1500 W m^{-2} in the Southern Ocean. The seasonal variability of FKEW is large, about 1600 W m^{-2} , along the coast of Somalia in the northern Indian Ocean. The maximum monthly variability of the FKEW field averaged over each zone occurs during boreal summer. During the onset and withdrawal of monsoon, FKEW is as low as 50 W m^{-2} . The Southern Ocean has a large variation of about 1280 W m^{-2} because of strong westerlies throughout the year.

RÉSUMÉ [Traduit par la rédaction] Nous avons effectué une étude détaillée de la variabilité à long terme du vent, à partir de 30 ans de données de réanalyses mondiales atmosphériques (ERA-Interim) du Centre européen pour les prévisions météorologiques à moyen terme (ECMWF). L'étude couvre l'océan Indien, que nous avons divisé en six zones, selon les extrêmes locaux du vent. La tendance moyenne de la vitesse du vent moyen annuel, calculée pour chaque zone, montre une hausse significative dans la région équatoriale, dans l'océan Austral et dans la partie sud des alizés. Ces résultats indiquent que les vents de l'océan Austral et les alizés du sud-est forcent. Toutefois, la tendance est négative sur le golfe du Bengale. Un affaiblissement des vents de mousson et des alizés du nord-est pourrait causer cette baisse. La variabilité interannuelle maximale survient dans la mer d'Oman en raison de la mousson. Nous observons un minimum dans la région subtropicale, dû à la divergence des vents. Les variations de la vitesse du vent, pour toutes les zones, sont faiblement corrélées avec l'indice du dipôle de l'océan Indien. Toutefois, l'océan Indien équatorial, la partie sud des alizés et les zones subtropicales montrent une corrélation positive relativement forte avec l'indice d'oscillation australe. Ce lien indique que l'oscillation australe influe de façon zonale sur la vitesse du vent dans l'océan Indien. Les vents de mousson montrent une tendance à la baisse dans la partie nord de l'océan Indien; ce résultat indique un affaiblissement de la mousson. Par contre, ils présentent une tendance à la hausse dans la région équatoriale, due au renforcement des vents d'ouest. La tendance négative que nous observons durant les périodes sans mousson pourrait être le résultat d'un affaiblissement des alizés du nord-est au cours des dernières décennies. Le flux moyen de l'énergie cinétique du vent atteint un minimum d'environ 100 W m^{-2} dans la région équatoriale et un maximum d'environ 1500 W m^{-2} dans l'océan Austral. La variabilité saisonnière de ce flux est forte, environ 1600 W m^{-2} , le long du littoral somalien et dans le nord de l'océan Indien. La moyenne de la variabilité maximale mensuelle du flux de l'énergie cinétique du vent, calculée pour chaque zone, survient durant l'été boréal. Au début et à la fin de la mousson, le flux peut chuter à 50 W m^{-2} . L'océan Austral présente une grande variation, 1280 W m^{-2} , en raison des forts vents d'ouest qui soufflent toute l'année.

*Corresponding author's email: mony@nio.org

KEYWORDS Indian Ocean; monsoon; long-term trend analysis; trade winds; ENSO; Indian Ocean Dipole; flux of kinetic energy of wind

1 Introduction

Surface wind is the fundamental variable in air–sea interaction processes. Analysis of long-term wind has been carried out by several researchers using various techniques (Bauer, 1996; Caires & Sterl, 2005; Gulev & Grigorieva, 2004; James, Holton, Curry, & Pyle, 2003; Källberg et al., 2005; Monahan, 2006; Phillips, 1977; Young, Vinoth, Zieger, & Babanin, 2012). Lledó, Dubois, Barton, and Brower (2013) used different global datasets to study wind speed variability and found that winds from the European Centre for Medium-range Weather Forecasts (ECMWF) global atmospheric reanalysis (ERA-Interim) correlate well with observations, and the interannual variability agrees well with observations ($r^2 \approx 0.80$). These studies indicate the variability of surface winds over a period of time. Wind speed data collected from ships in the South China Sea, North Pacific Ocean, and North Atlantic Ocean were analyzed by Cardone, Greenwood, and Cane (1990) who showed that the trends have strengthened over the past few decades. Studies of wind variability carried out globally show positive trends throughout the years, whereas temporal studies carried out at a few locations, such as the subtropical North Pacific, south of Green Island, and the tropical South Atlantic, show negative trends (Tokinaga & Xie, 2011). The negative trends in the subtropical North Pacific have been attributed to a reduction in the northeast trade winds and are consistent with global warming simulations (Xie et al., 2010). Gower (2002) observed positive as well as negative wind speed trends in data from various buoys across the North Pacific. Thomas, Kent, Swail, and Berry (2008) observed a positive wind speed trend of about $0.10 \text{ m s}^{-1} \text{ decade}^{-1}$ using the International Comprehensive Ocean Atmosphere Data Set. Young, Zieger, and Babanin (2011) analyzed satellite altimeter measurements and found that the rate of increase is greater for extreme events than for the mean. Zieger, Babanin, and Young (2014), using altimeter data from 1991 to 2008, found that the global trend is not uniformly distributed, and in some regions the trends were nearly two times greater than the global average trend.

The Indian Ocean basin has been studied by many researchers (Cai & Cowan, 2013; Dong, Tianjun, & Bo, 2014; Saji, Goswami, Vinayachandran, & Yamagata, 1999; Zheng et al., 2013), considering either the entire ocean or part of it as the domain. In this regard, only a few researchers have been able to carry out a detailed analysis of wind and wave dynamics in the Indian Ocean. Polnikov, Pogarskii, and Sannasiraj (2011) and Pogarskii, Polnikov, and Sannasiraj (2012) analyzed 12 years of reanalysis data from the National Centers for Environmental Prediction/National Center for Atmospheric Research (NCEP/NCAR) (<ftp://polar.ncep.noaa.gov/pub/history/waves/>) and observed interesting features of the wind fields by partitioning the Indian Ocean into zones of independent wind dynamics, estimating extrema

and mean values at the central points of each zone, and analyzing statistical and spectral characteristics of the winds in detail. Rashmi et al. (2014) studied decay rates and variance of wind fields using spectral analysis of time series of ERA-Interim data for the 1979–2012 period at the central point of each zone. Bhaskaran, Gupta, and Dash (2014) studied the trend in wind speed over the Indian Ocean using satellite observations for a period of 21 years from 1992 to 2012. They found that the highest variability occurred in the Southern Ocean belt because of the impact of climate change. However, mapping of the wind field and subjecting long-term (30 years) wind data to statistical and spectral analyses has not been done for the Indian Ocean. In this context, the authors have made an attempt to study the spatiotemporal features of the wind field, wind energy, statistics, and long-term trends using ERA-Interim data (<http://apps.ecmwf.int/datasets/data/interim-full-daily/levtype=sfc/>).

We divided the Indian Ocean into six zones based on the characteristics of the wind-field dynamics. This allows us to detect wind-field variability separately in each zone and provides greater certainty and finer detail than earlier studies (Caires & Sterl, 2005; Gulev & Grigorieva, 2004; Källberg et al., 2005; Monahan, 2006; Pogarskii et al., 2012). In our study, we carried out detailed analyses of annual, seasonal, and 90th and 99th percentile trends, interannual variability and Weibull probability density functions (PDFs) of wind speed averaged over each zone, and estimated the mean flux of kinetic energy of wind (FKEW) field and its annual trend, as well as the seasonal and monthly variability over each zone to understand the variability in each zone (rather than considering one point at the centre of each zone as in previous studies).

2 Data and methodology

The wind field, $W(x,y,t)$ at 10 m height for the Indian Ocean with a spatial resolution of $1.5^\circ \times 1.5^\circ$ in latitude and longitude and a temporal resolution of 6 hours was obtained from the ERA-Interim global atmospheric reanalysis database; ERA-Interim is a third-generation reanalysis dataset that uses a much improved atmospheric model and assimilation system than those used in the 40-year reanalysis dataset from ECMWF (ERA-40). The data assimilation system used to produce ERA-Interim is based on the 2006 release of the Integrated Forecast System (Cy31r2). This system includes a four-dimensional variational analysis (4D-Var) with a 12-hour analysis window. The spatial resolution of the dataset is approximately 80 km (T255 spectral) on 60 vertical levels from the surface up to 0.1 hPa. Observations assimilated in ERA-Interim and their sources are described in Uppala et al. (2005). The dataset is physically and dynamically coherent. Recently, several sections of the dataset

have been improved, such as the low frequency variability, analysis accuracy, hydrological cycle, and quality of the stratospheric circulation (Dee et al., 2011).

The accuracy of ERA-Interim winds was assessed by comparing its wind data with wind data from a moored buoy deployed in the Bay of Bengal, as well as with the NCEP/NCAR wind dataset. The comparison of the buoy wind data with ERA-Interim and NCEP/NCAR winds is shown in Fig. 1; the agreement with the ERA-Interim wind dataset is better than with the NCEP/NCAR wind dataset, as shown by the statistics (root mean square error (rmse) = 1.27 m s⁻¹ and 1.97 m s⁻¹, respectively; bias = 0.05 m s⁻¹ and 0.24 m s⁻¹, respectively; correlation coefficient = 0.77 and 0.58, respectively). However, in extreme events, the reanalysis wind underestimates the buoy wind.

We have analyzed the wind speed time series obtained from the ERA-Interim dataset for the Indian Ocean over a period of 30 years for mean wind speed, mean annual spatial and temporal trends for zonal and meridional winds, as well as wind speeds, over each zone, extremes, seasonal and interannual variability averaged over zones, and the temporal variability of the Weibull PDF.

In order to analyze wind energy, mean densities of FKEW, $\langle E_A(i, j, T) \rangle$, were calculated using the formula

$$\langle E_A(i, j, T) \rangle = \left(\sum_{t_n \in T} \Delta t_n \rho_a W^3(i, j, t_n) / 2 \right) / \sum_{t_n \in T} \Delta t_n. \quad (1)$$

where Δt_n is the time step for the wind field; T is the averaging period; $W(i, j, t_n)$ is the wind module at the spatial node (i, j) at time t_n ; $\rho_a = (353/T_K)$ kg m⁻³ is the air density, which depends on temperature T_K (Kelvin) and varies with latitude and season (Källberg et al., 2005). The purpose of this task is to estimate the quantitative spatial distribution of FKEW over the entire Indian Ocean, its seasonal, annual, and decadal variation, and to determine the 30-year trend. The units of FKEW are given as power per unit area perpendicular to the wind

direction (Watts per square metre). The significance of FKEW lies in the fact that it is the actual physical field that provides the rate of mechanical energy transfer from the wind to the waves (Golitsyn, Polnikov, & Pogarskii, 2012; Phillips, 1977). Thus, having reference values of mean extremes and trends for FKEW, we will be able to focus more on the dynamics of the atmosphere–ocean mechanical interactions.

3 Results and discussion

a The Mean Wind Field

Typical mean zonal (u) and meridional (v) wind components, as well as wind speed over a period of 30 years (1980–2010), were computed and are shown in Fig. 2. The 30-year mean zonal wind component has a maximum speed of 9.5 m s⁻¹ (westerlies) in the Southern Ocean and 7.5 m s⁻¹ between 10° and 30°S. The meridional wind component has a maximum speed of 6 m s⁻¹ (southerlies) between 10° and 30°S and a minimum in the Southern Ocean. The 30-year mean wind speed clearly shows the zonal structure. The winds are weaker (minimum mean wind speed = 3 m s⁻¹) along the equatorial zone and stronger (maximum mean wind speed = 12.5 m s⁻¹) between 40° and 60°S.

Figure 2 shows a clear and stable spatial distribution of the wind speed. The Indian Ocean was divided into the following six zones, considering the presence of a local extrema in the wind field: the Arabian Sea – Z1, the Bay of Bengal – Z2, the equatorial part of the Indian Ocean – Z3, the southern part of the trade winds – Z4, the southern subtropical part of the Indian Ocean – Z5, and the southern Indian Ocean – Z6. The distribution of wind-field extremes with different time averaging scales indicates the stability of the spatial dynamics of the atmospheric circulation over the entire Indian Ocean. The zones shown in Fig. 3 cover all the geographical features of the Indian Ocean: coastal boundaries (Z1, Z2), typical large-scale zonal distribution of global air circulation, namely, zones of the trade winds and the Southern Ocean (Z4, Z6), and the equatorial and subtropical zones (Z3, Z5).

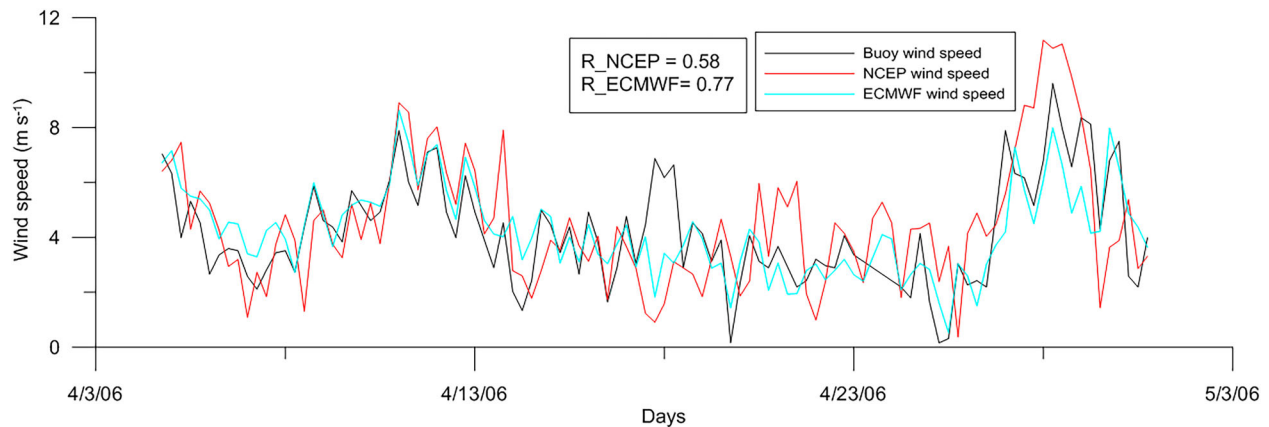


Fig. 1 Temporal plot of buoy wind speed (in the Bay of Bengal; black), ERA-Interim wind speed (blue), and NCEP/NCAR wind speed (red). The correlation coefficients of buoy wind speed with ERA-Interim and NCEP/NCAR wind speeds are 0.77 and 0.58, respectively.

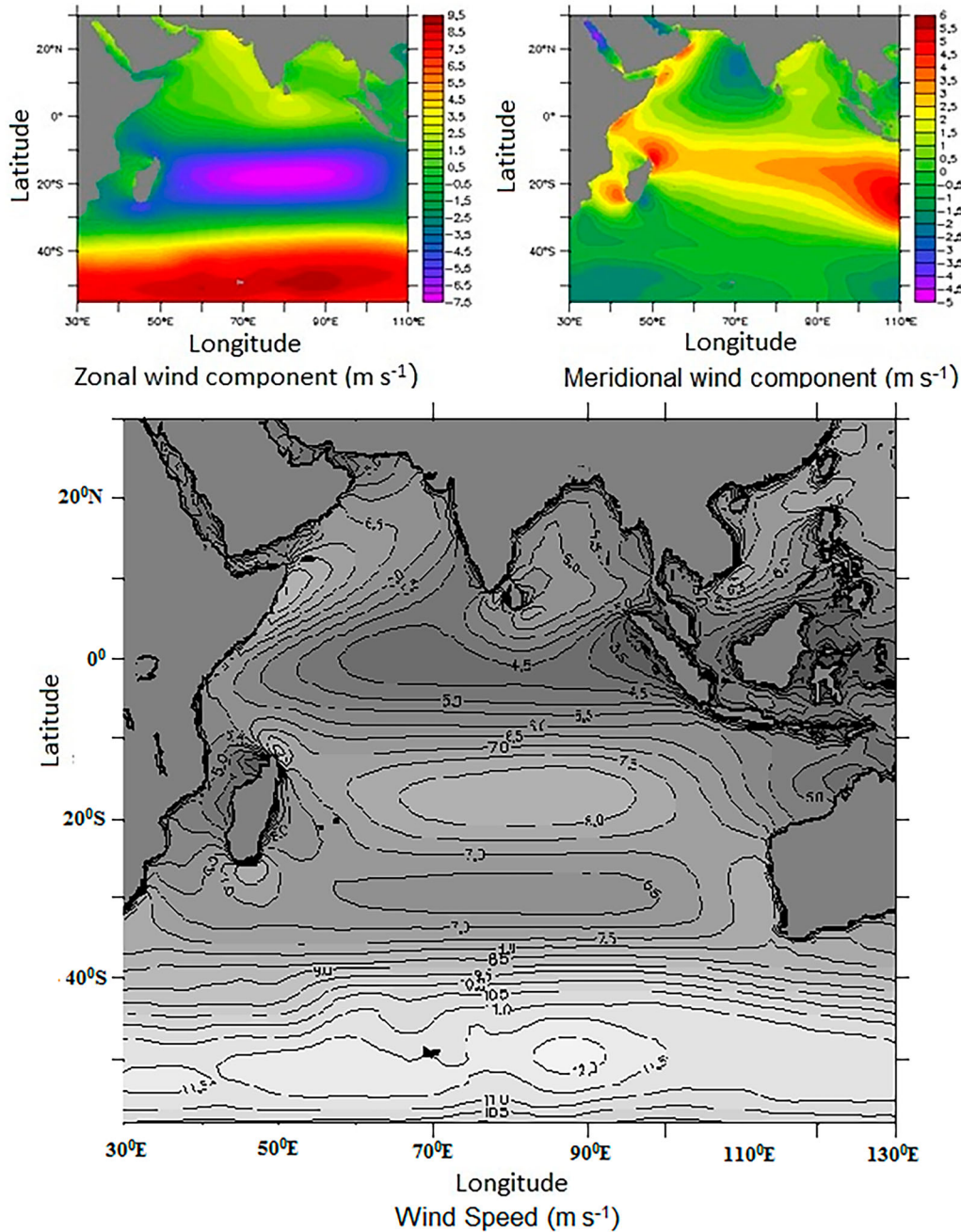


Fig. 2 Mean zonal (u) and meridional (v) wind components and wind speed (m s^{-1}) over the Indian Ocean for the 1980–2010 period.

The conventional boundaries of the zones and the locations of their “central” points are shown in Fig. 3 by thick straight lines and black squares, respectively. It is shown that the statistical properties of the wind field in all these zones are quite different, and this will be studied separately.

The 30-year annual-mean trends of the zonal and meridional winds, as well as the wind speed, were obtained spatially and are shown in Fig. 4. Wind speed trends averaged over each zone are presented in Table 1.

The temporal trend obtained using a least square fit for each point of the annual-mean wind field for the entire Indian Ocean

is presented in Fig. 4. It is characterized by chaotic heterogeneity, with little correspondence to the zonal structure shown in Fig. 3. The positive trend of the annual-mean wind speed is of the order of $0.04 \text{ m s}^{-1} \text{ y}^{-1}$, found mainly in zone Z3. Areas of weak negative trends, on the order of $-0.042 \text{ m s}^{-1} \text{ y}^{-1}$, are seen along the central coast (of India) of zones Z1 and Z2, as well as in the eastern and western parts of zone Z6. The annual maximum zonal wind component trend of about $0.048 \text{ m s}^{-1} \text{ y}^{-1}$ is observed in the middle of the Southern Ocean (Z6) and the maximum meridional trend of about $0.042 \text{ m s}^{-1} \text{ y}^{-1}$ along the coasts of Sumatra and Somalia.

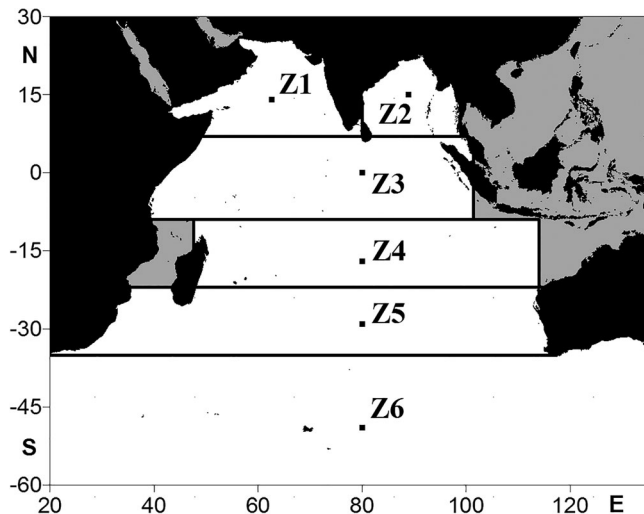


Fig. 3 Zonal structure and location of central points of the zones in the Indian Ocean (no significance is attached to central points; used only for computation and discussion).

Statistical reliability of the established trend is small ($r^2 = 0.09$), and the values of the trend are within the confidence intervals estimated above.

Further, the wind field was averaged over each zone, and the 30-year mean annual trend was obtained using moving average values spanning three years. The mean annual trends along with the 95% confidence intervals for all the zones are given in Table 1. The significance is determined using a Student's *t*-test, which clearly indicates strong wind activity in zones Z4 and Z6 and weak wind activity in zone Z2. This shows that the wind speed trend of the westerlies in Z6 have strengthened over the period. The trend in the equatorial zone is stronger than in all the other zones. In zone Z4, the southeasterly trade winds are strengthened significantly.

The seasonal difference in the 30-year mean wind speed for all summers (July) and winters (January) is shown in Fig. 5a.

Summer is the most dynamically active of all the seasons. Wind speeds are higher in the northern zones (up to $5\text{--}6\text{ m s}^{-1}$ or 50% of the summer values) and lower in the southern zones of the Indian Ocean (less than 4 m s^{-1} or 30%) because of monsoon activity in the northern zones. The negative value of the seasonal difference is noticeable near the western coast of Australia, reaching 2 m s^{-1} (about 50%). Another interesting feature is an increase in the trade winds (up to 4 m s^{-1}) during summer.

Recently, Rao et al. (2012), Roxy, Ritika, Terray, and Masson (2014), and Swapna, Krishnan, and Wallace (2014) noticed a drastic increase in the equatorial warming trend in the Indian Ocean over the past few decades, accompanied by a pronounced weakening of the large-scale boreal summer monsoon circulation. Further, Sandeep and Ajayamohan (2014) observed a poleward shift in the monsoon low-level jet stream. In this context, we have made an attempt to analyze trends during monsoon (June, July, August, and September; JJAS) and non-monsoon (January, February, March,

and April; JFMA) winds in zones Z1, Z2, and Z3, where the influence of monsoons is strong. The trends in southwest monsoon winds from June to September and non-monsoon winds from January to April were analyzed and are shown in Fig. 5b. During the monsoon period (Fig. 5b(i)), a decrease in the annual-mean wind speed trend can be seen in zones Z1 and Z2, whereas an increase is observed in zone Z3. This is consistent with the recent studies noted above, indicating a weakening of monsoon in the northern part of the Indian Ocean as the flow of southwesterly winds is reduced. However, the increasing trend in zone Z3 indicates an enhancement of the westerly winds (Swapna et al., 2014). As shown in Fig. 5b(i), a similar type of variation is noticeable for non-monsoon winds (Fig. 5b(ii)). During the non-monsoon period, northerly to northeasterly winds prevail over the northern part of the Indian Ocean. This shows that the northeast trade winds have weakened in recent decades, as observed by Xie et al. (2010) in the North Pacific.

In order to see the variability in extreme winds, 90th and 99th percentile wind speeds averaged over each zone were analyzed, and the corresponding trend values are reported in Table 1. A positive trend is seen in zones Z3 and Z5, whereas the remaining zones show trends of opposite signs for both the 90th and 99th percentiles. A strong positive trend in the 90th percentile wind speed is observed in zones Z3 and Z5, whereas a negative trend is observed in zones Z2 and Z4. However, zones Z1, Z2, Z3, and Z5 show a strong positive trend at the 99th percentile, and zones Z4 and Z6 show a strong negative trend. The annual mean of the southeasterly trade winds and westerlies in zones Z4 and Z6 increase strongly in comparison with the extreme wind speeds. The northern Indian Ocean (i.e., zones Z1 and Z2) shows a strong increase in the 99th percentile wind speeds because of monsoon activity in zone Z1 and also because of significant cyclonic activity in zone Z2. However, zone Z5 consistently shows an increase in both extremes and annual-mean wind speeds.

Further, the interannual variability of wind speed (Fig. 6) shows a very interesting intermittent structure. The interannual signal shows a standard deviation of 1.15 m s^{-1} . The distinct zone-wise variation in wind speed is very evident in the analysis.

All the zones show substantial interannual variability in mean annual wind speeds (Fig. 6) although the standard deviation at some points is remarkably constant. The maximum deviation is observed in zone Z1 and the minimum in zone Z5 because of the strong seasonal variation in zone Z1, whereas in zone Z5, wind divergence is strong and the deviation is lower throughout the year. All other zones show similar variations throughout the year.

As a result of equatorial warming in the Indian Ocean over the last few decades, continental heating during boreal summer has led to a strong meridional pressure gradient that drives the southwest monsoon (Han et al., 2014). The intense monsoon winds induce a strong northward Somali Current and coastal upwelling near the coasts of Somalia

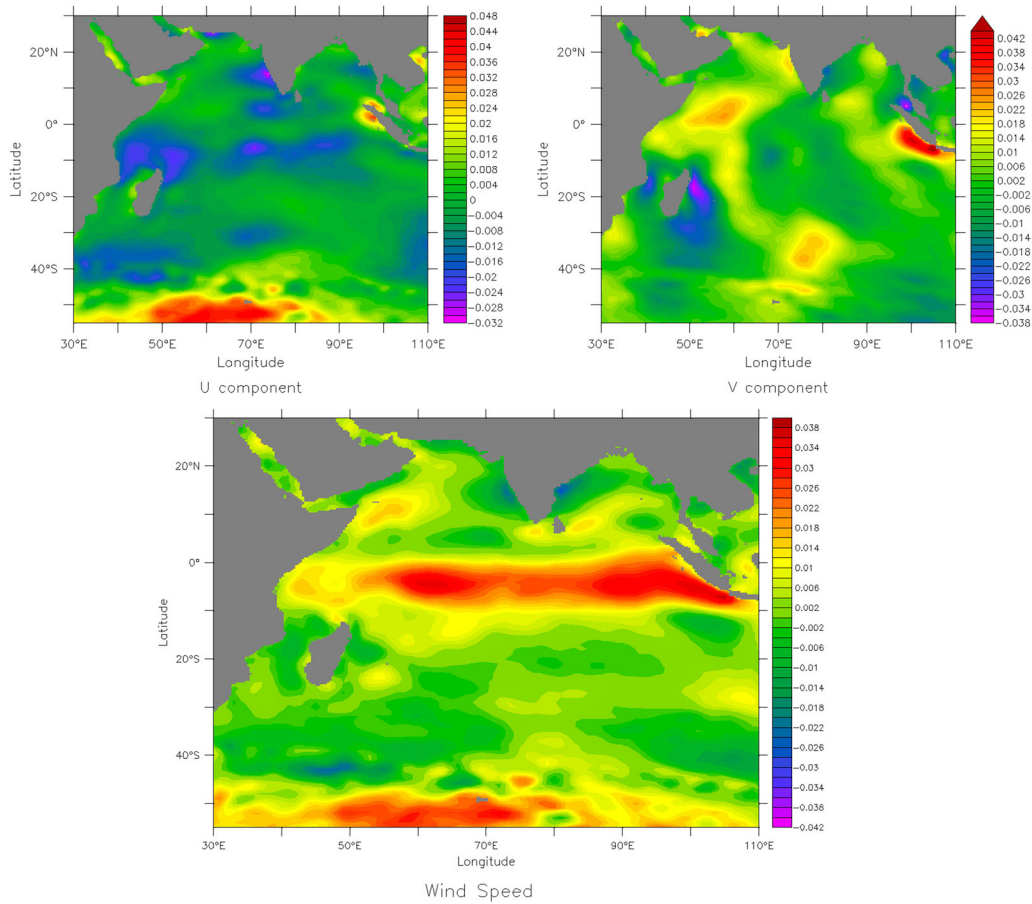


Fig. 4 Trends ($\text{m s}^{-1} \text{y}^{-1}$) in annual-mean zonal and meridional winds and annual-mean wind speed for the 30-year period.

and Oman (Figs 2b and 2d in Han et al., 2014). During the winter monsoon, surface winds (Fig. 2a in Han et al., 2014) and ocean circulation (Fig. 2c in Han et al., 2014) reverse direction across the entire basin north of 10°S. In contrast, south of 10°S, the South Equatorial Current flows westward throughout the year under the influence of relatively steady trade wind forcing. Ocean–atmosphere interactions in the Indian Ocean can also give rise to significant climate fluctuations. As with the El Niño–Southern Oscillation (ENSO), the Indian Ocean Dipole varies on interannual time scales, sustained through positive feedbacks between equatorial winds and zonal sea surface temperature (SST) gradients. The

zonal wind anomaly along the equator drives the upper ocean response, which is closely related to the interannual SST difference across the tropical Indian Ocean (Feng & Meyers, 2003). Interannual variability in the equatorial Indian Ocean is highly dependent on equatorial zonal wind changes (Sreenivas, Gnanaseelan, & Prasad, 2012). Decadal sea level variations in the Bay of Bengal are strongly related to zonal wind variations over the central and eastern equatorial Indian Ocean (Nidheesh, Lengaigne, Vialard, Unnikrishnan, & Dayan, 2013).

From previous studies it can be seen that interannual and decadal variations in the northern Indian Ocean are strongly

TABLE 1. Trends in annual-mean wind speed, as well as the 90th and 99th percentiles for all zones. The 95% confidence interval is shown in parentheses.

Zones	Trends ($\text{m s}^{-1} \text{y}^{-1}$)		
	Mean	90th percentile	99th percentile
Z1	0.0015 (−0.0008, 0.0038)	−0.0005 (−0.0077, 0.0067)	0.0061 (−0.0062, 0.0185)
Z2	−0.0008 (−0.0032, 0.0016)	−0.0041 (−0.0138, 0.0057)	0.0043 (−0.0093, 0.0179)
Z3	0.0129 (0.0109, 0.0150)	0.0071 (0.0011, 0.0132)	0.0088 (0.0019, 0.0158)
Z4	0.0036 (0.0014, 0.0058)	−0.0035 (−0.0104, 0.0034)	−0.0026 (−0.0123, 0.0071)
Z5	0.0014 (−0.0012, 0.0040)	0.0022 (−0.0036, 0.0079)	0.0017 (−0.0065, 0.0099)
Z6	0.0046 (0.0014, 0.0078)	0.0002 (−0.0073, 0.0076)	−0.0043 (−0.0140, 0.0055)

related to equatorial zonal wind changes. Correlation coefficients between wind speed averaged over each zone and the Southern Oscillation Index (SOI) and the Dipole Mode Index (DMI) are presented in Table 2. As seen in Table 2, the wind speed variations in all zones are weakly correlated with DMI. However, the equatorial Indian Ocean (Z3), the southern part of the trade winds (Z4), and the subtropical (Z5) zones show a relatively strong positive correlation with SOI. This shows that the influence of ENSO is larger in the equatorial and subtropical zones. In the southerly trade winds zone (Z4), cyclones form frequently because of the strong influence of the SOI in this zone. Warming in the equatorial Indian Ocean has a stronger influence in the Arabian Sea zone (Z1) (as seen by the positive correlation with SOI) than in the Bay of Bengal zone (Z2). This clearly indicates that SOI has a zonal influence on wind speed in the Indian Ocean.

b The Flux of Kinetic Energy of Wind

The importance of studying FKEW lies in the fact that it determines the rate of mechanical interaction between the

atmosphere and the ocean (Golitsyn et al., 2012; Phillips, 1977). Additional specificity for estimating the FKEW field is provided by considering the air-density dependence on temperature, $\rho_a(T_K)$, defining $\langle E_A(i, j, T) \rangle$ (Eq. (1)), which varies with season and latitude. This is based on the temperature variability data in an ECMWF report (Kållberg et al., 2005). To our knowledge, there is only one analogue (Pogarskii et al., 2012) in which such calculations and analyses have been performed using the NCEP/NCAR wind field over the Indian Ocean. In this work, we have carried out a more detailed study of the FKEW field over the Indian Ocean by using ERA-Interim over a period of 30 years (Figs 7 and 8).

TABLE 2. Correlation coefficients between wind speed averaged over each zone and climate indices.

WS/Zones	Z1	Z2	Z3	Z4	Z5	Z6
DMI	-0.12	0.01	-0.06	-0.07	-0.24	0.20
SOI	0.22	0.10	0.51	0.32	0.54	-0.01

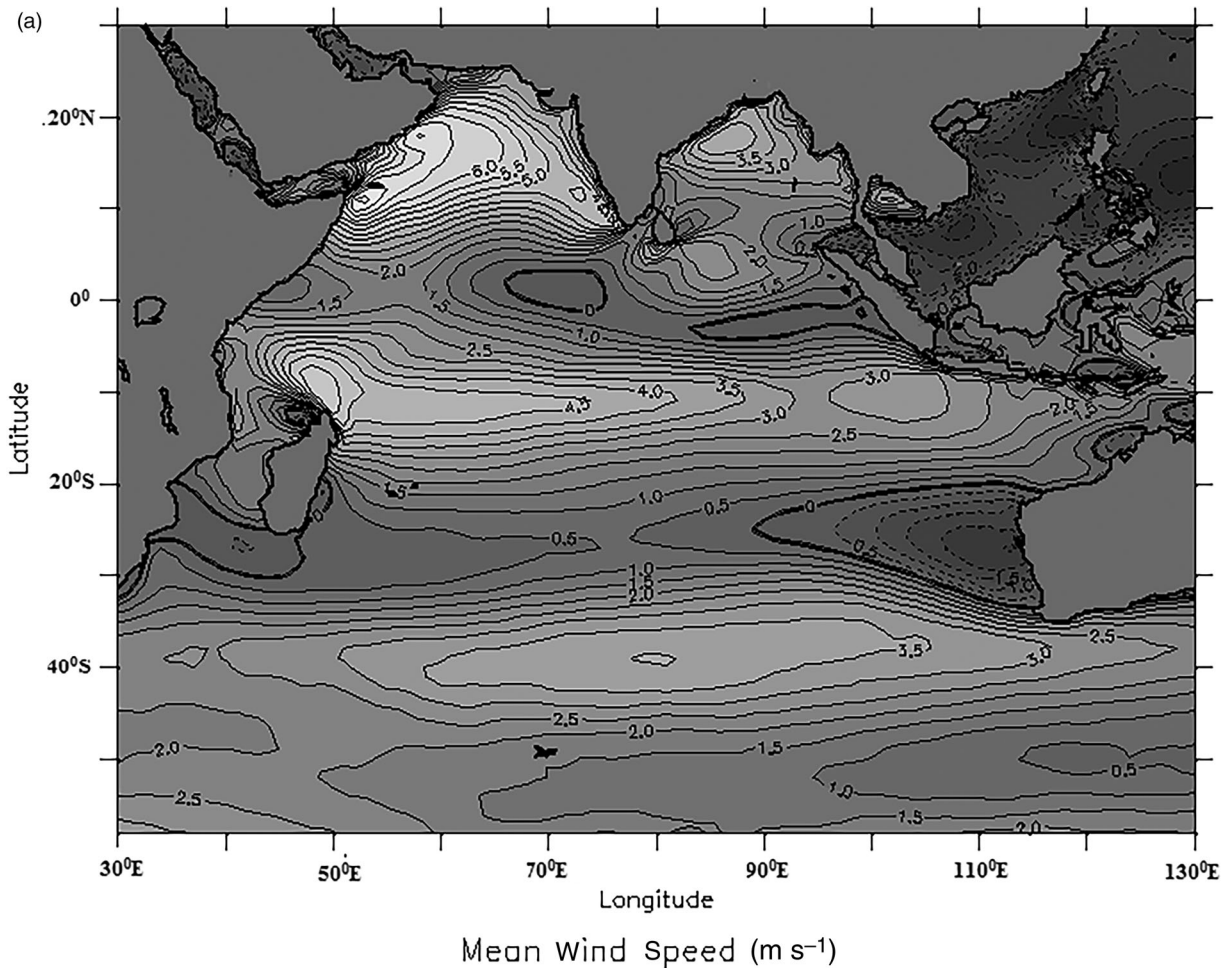


Fig. 5 (a) Seasonal difference in 30-year mean wind speed ($m s^{-1}$) between summer (July) and winter (January). (b) Annual-mean trend in wind speed ($m s^{-1}$) during (i) the monsoon period (JJAS) and (ii) the non-monsoon period (JFMA).

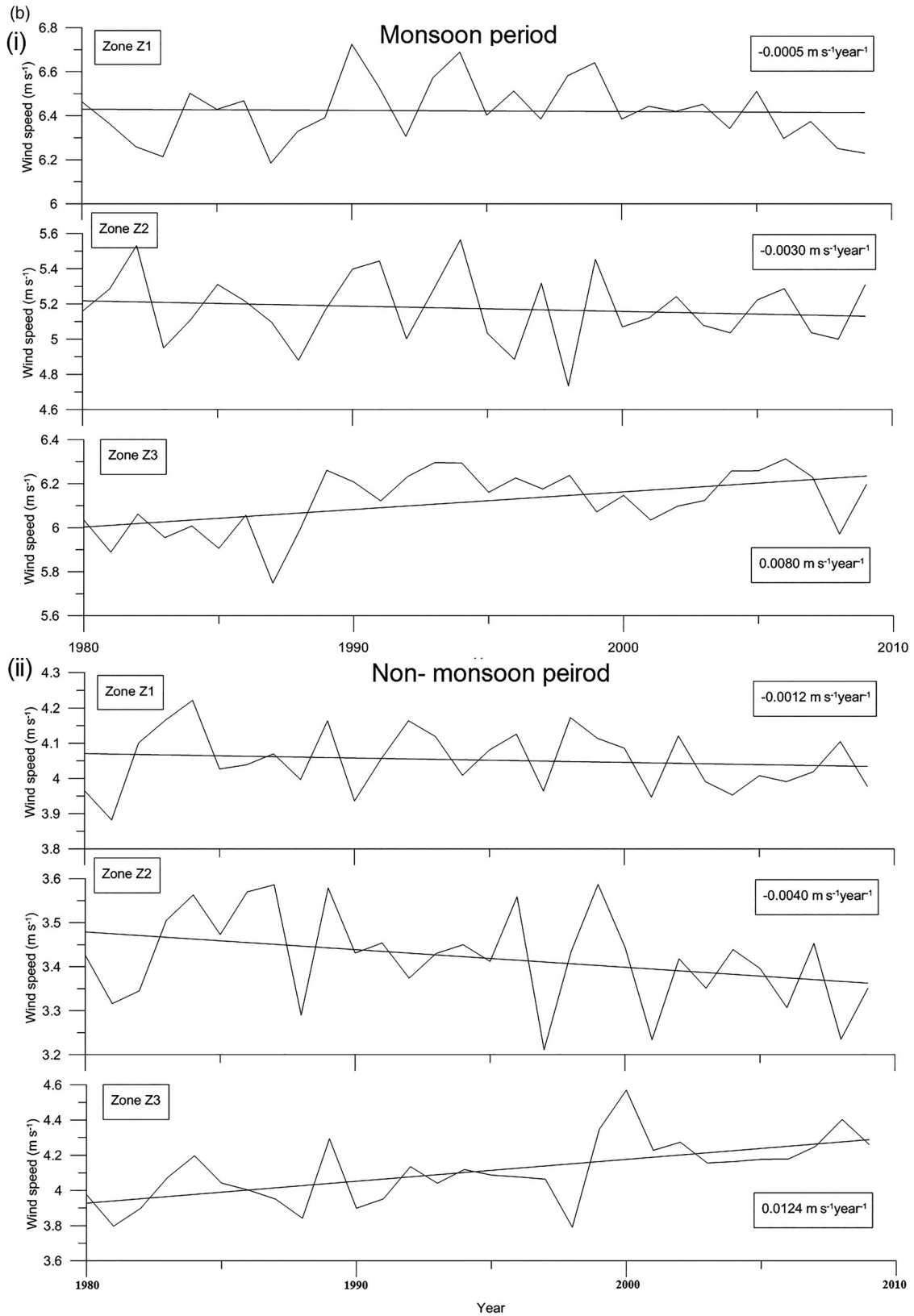


Fig. 5 Continued

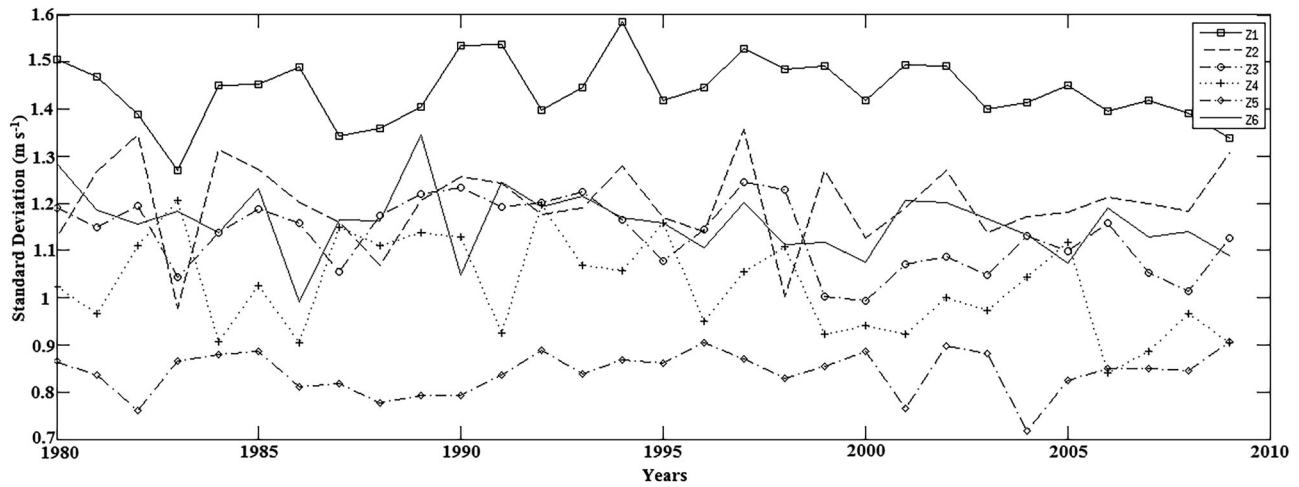


Fig. 6 30-year interannual variability of wind speed (m s^{-1}).

The 30-year mean FKEW field is shown in Fig. 7. The comparison of FKEW values of ERA-Interim reanalysis with the values using NCEP/NCAR data (Pogarskii et al., 2012) shows a reduction in the former (15%) with respect to the latter. Therefore, we find that the FKEW field is a real physical characteristic of the wind field that is suitable for the study of wind-field spatial

variability. The zonal structure is well expressed in Fig. 7 — a minimum of about 100 W m^{-2} (in Z3) and a maximum of about 1500 W m^{-2} (in Z6). The range of FKEW variability averaged over the entire period reaches 12 (actual units), while the range for the mean wind-speed field is about 3 (actual units). Therefore, the FKEW field is more suitable than the wind

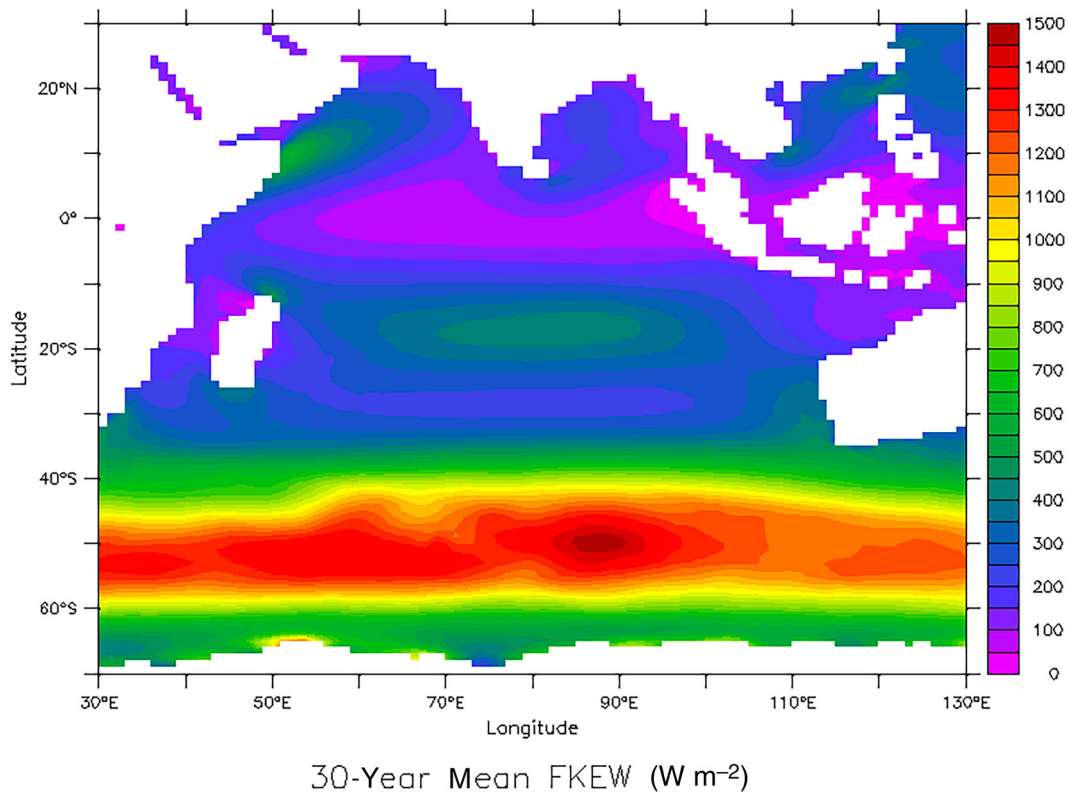


Fig. 7 30-year mean FKEW field (W m^{-2}) calculated for the Indian Ocean.

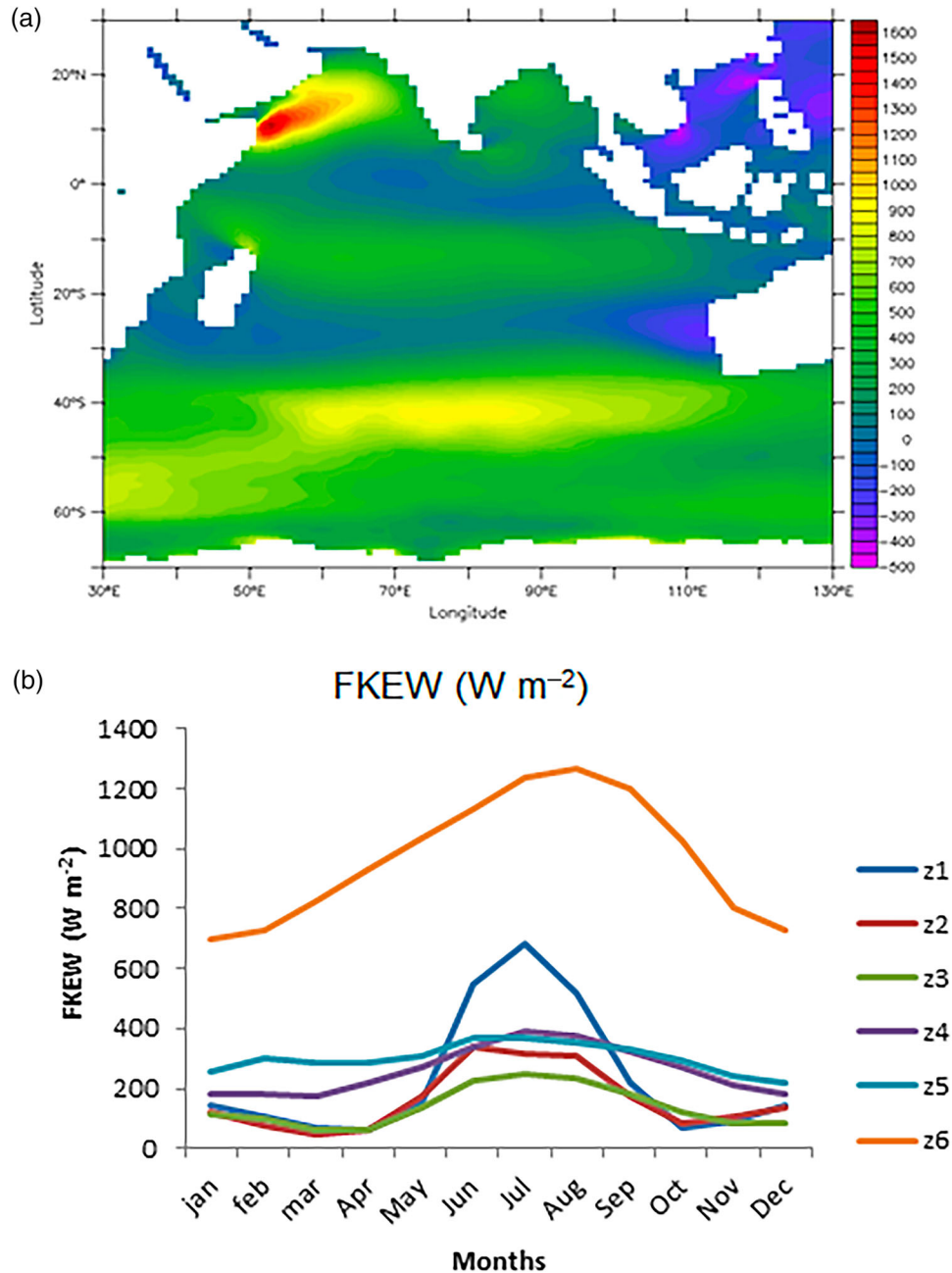


Fig. 8 (a) 30-year mean seasonal difference (July–January) in the FKEW field (W m^{-2}) and (b) monthly variability of the FKEW field (W m^{-2}) averaged over each zone.

speed field for the detailed study of the horizontal distribution at large (geophysical) scales. Thus, the FKEW field is found to be a good marker of spatiotemporal variability and is one of the useful results to emerge from our analysis.

The 30-year seasonal variability of FKEW is shown in Fig. 8a. The seasonal difference is well expressed and has a maximum value of about 1600 W m^{-2} in Z1. The large seasonal difference is a result of strong monsoon activity along the coast of Somalia in the northern Indian Ocean. In order to understand

the flux variation in detail, the monthly variability of FKEW was determined (Fig. 8b). Zones Z6 (maximum of about 1280 W m^{-2}) and Z3 (maximum of about 250 W m^{-2}) show the maximum and minimum variability of FKEW, respectively (Fig. 8b). However, large variability is observed during boreal summer in zones Z1, Z2, and Z3. During boreal summer, the Arabian Sea (Z1) has a maximum FKEW of approximately 690 W m^{-2} , which is higher than in zones Z2 and Z3 because of the stronger influence of monsoon activity in zone Z1 than

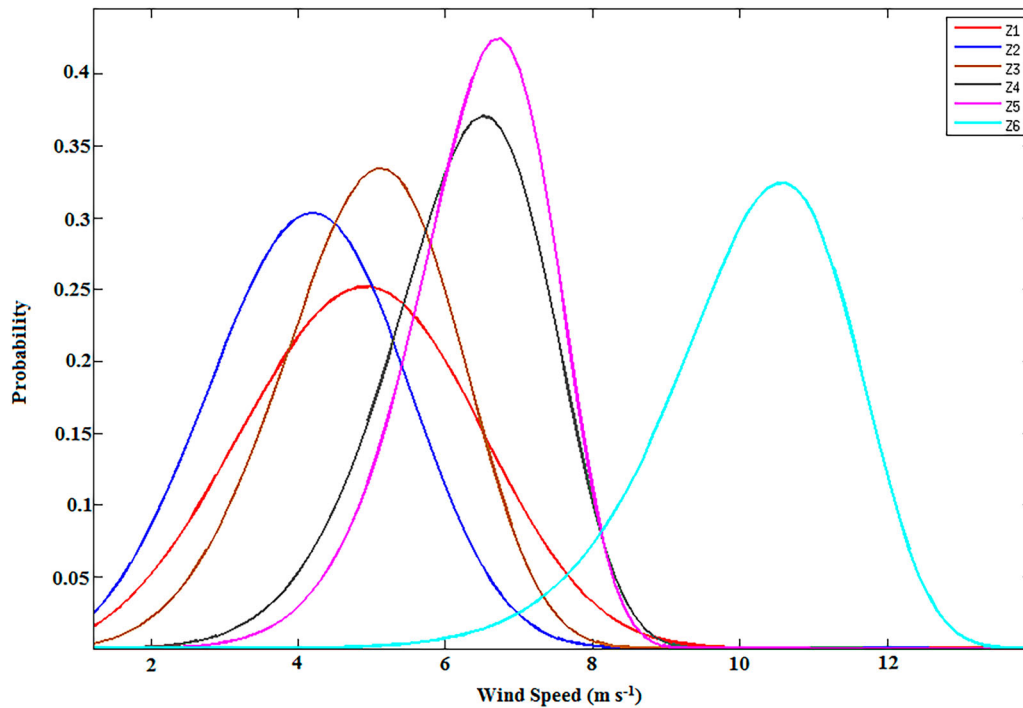


Fig. 9 Weibull PDFs for all zones with occurrence on the y-axis and wind speed (m s^{-1}) on the x-axis.

in other zones. During the onset and withdrawal of monsoon, FKEW is as low as 50 W m^{-2} . However, zones Z4 and Z5 do not show significant variation in the annual FKEW because there is no significant seasonal influence in these zones. The Southern Ocean (Z6) shows large variation because of strong westerlies (observed throughout the year). We found no significant change in the 30-year annual-mean FKEW trend (figure not shown). However, the temporal variation of FKEW averaged over each zone shows an increasing trend in all zones, except the Bay of Bengal (Z2).

c Distribution Function

The unimodal, two-parameter Weibull PDF has been found to be closely related to surface wind speed distribution (Justus, Hargraves, & Yalcin, 1976) and is widely used for long-term surface wind speed studies (Monahan, 2006; Klink, 2007; Yan, Bate, Chandler, Isham, & Wheatler, 2002). The Weibull PDFs of mean daily wind speed, averaged over

each zone, are shown in Fig. 9 for all zones. The PDFs generated using the Weibull scale a and shape b values with the 90% confidence intervals are given in Table 3. Parameter a is a function of mean wind speed averaged over each zone and describes the central tendency, whereas b describes the peakedness of the distribution. Parameter, a ranges from 4.58 m s^{-1} in zone Z2 to 10.69 m s^{-1} in zone Z6, and parameter b has a minimum of 3.54 in Zone Z1 and a maximum of 9.37 in zone Z6. The large value of parameter a corresponds to high mean wind speeds. The PDFs of mean daily wind speed over all zones show different characteristics. When the scale is wider, the peak is low and broad; otherwise, high and narrow peaks are observed. Maximum peakedness is observed in zone Z5 and the minimum is observed in zone Z1. All other zones have nearly similar distributions, with a shift in the scale.

In order to understand the behaviour of these distributions, wind speed histograms with Weibull PDFs for all zones were prepared (Fig. 10). The data were divided into 45 equally spaced wind speed bins to generate the histograms. The wind speed scale is relatively broader with a bimodal structure for zone Z1. The winds in zone Z1 are predominantly in the range of $2\text{--}6 \text{ m s}^{-1}$, but wind speeds ranging from 6 to 9.5 m s^{-1} are also present. The observed strong winds are a result of monsoon activity in zone Z1. The frequency of weak winds (2.5 to 5 m s^{-1}) is high with a having a maximum value of 3 m s^{-1} . The occurrence of high winds is a result of cyclonic activity in zone Z2. In zone Z3, a double peak is observed, similar to zone Z1, caused by the influence

TABLE 3. Weibull shape and scale parameters along with the 95% confidence interval.

Zones	Scale parameter a (m s^{-1})	Shape parameter b
Z1	$5.38 \leq 5.40 \leq 5.41$	$3.51 \leq 3.54 \leq 3.56$
Z2	$4.57 \leq 4.58 \leq 4.60$	$3.60 \leq 3.62 \leq 3.65$
Z3	$5.37 \leq 5.38 \leq 5.39$	$4.74 \leq 4.77 \leq 4.81$
Z4	$6.68 \leq 6.69 \leq 6.70$	$6.62 \leq 6.67 \leq 6.71$
Z5	$6.83 \leq 6.84 \leq 6.85$	$7.78 \leq 7.83 \leq 7.89$
Z6	$10.68 \leq 10.69 \leq 10.70$	$9.31 \leq 9.37 \leq 9.44$

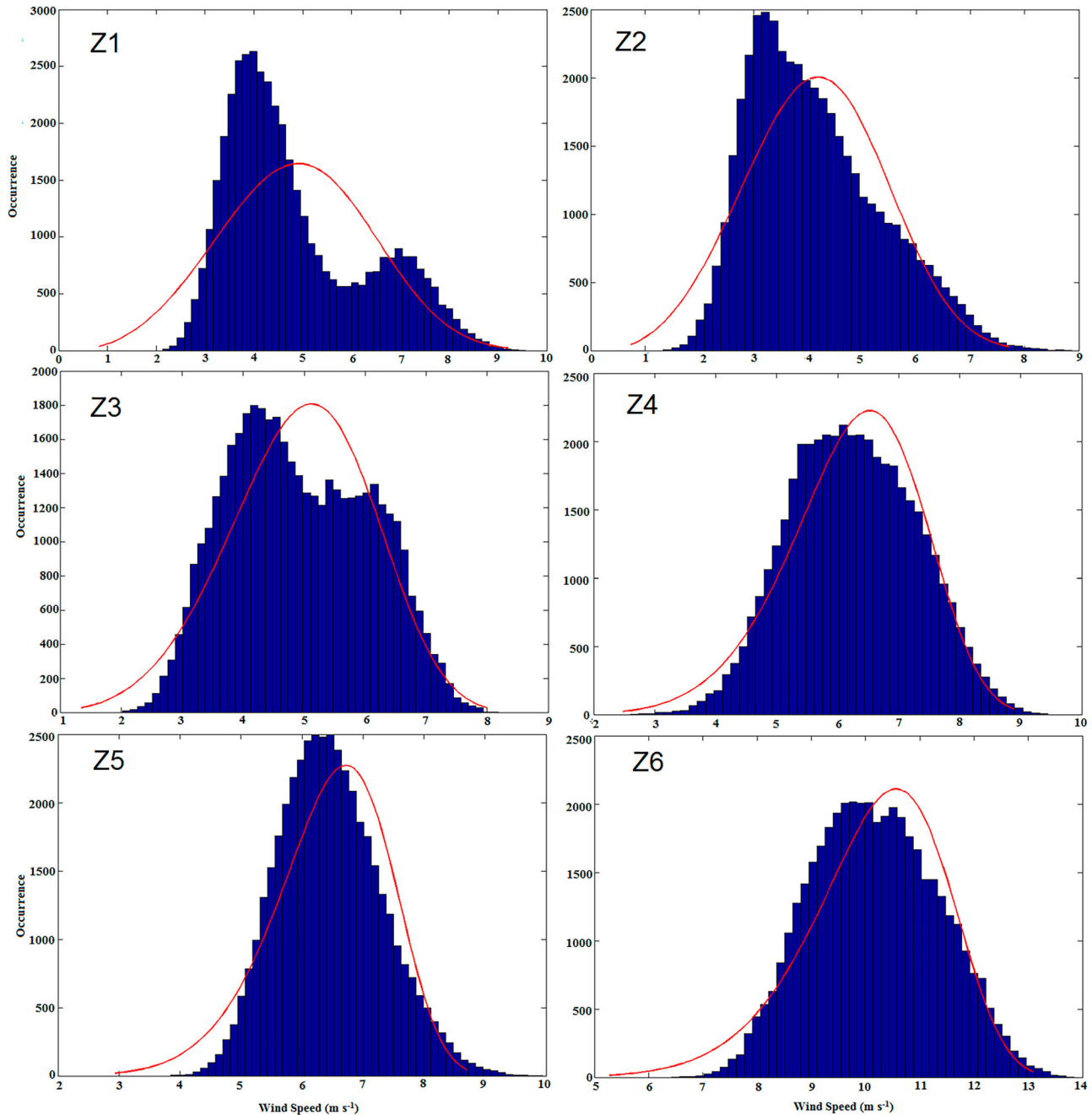


Fig. 10 Daily mean wind speed histogram (blue) and Weibull PDF (red) for all six zones in the Indian Ocean.

of monsoon activity occurring in zone Z3, confirmed by the strong flow of westerlies that are higher than in Z1. The Weibull PDF is a good fit (less exceedence) for trade winds in zone Z4 with a maximum value of a of 6 m s^{-1} . The wind speed distribution range in zone Z5 is narrow with a high peak. The Weibull curve is characterized by steeper slopes, a narrow range, and high winds in zone Z5. A strong shift in the range of the wind speed scale is seen in zone Z6 but not in other zones.

4 Conclusions

We have analyzed the wind and wind energy fields over the Indian Ocean for the 1980–2010 period. The 30-year mean wind speed has a zonal structure. The mean annual trend is almost neutral in zone Z2; however, the 99th percentile wind speeds experience a strong increase because of the frequency of cyclones in zone Z2. A strong positive trend in mean annual wind speed is seen for zone Z6, but the 90th percentile wind speed trend is almost neutral and the 99th

percentile wind speed trend decreases significantly over the period. Zones Z3 and Z4 show a consistent increase in mean annual and 90th and 99th percentile trends. The interannual variability has a maximum deviation in zone Z1 and a minimum in Z5. The wind speed averaged over each zone is weakly correlated with DMI. However, the SOI is highly correlated with wind speed in zones Z3, Z4, and Z5. We analyzed the annual-mean series for wind speed and wind energy for the six zones and the entire Indian Ocean. No systematic trend was seen in either wind speed or FKEW. The 30-year seasonal variability of FKEW has a maximum of about 1600 W m^{-2} in Z1. The monthly variability of FKEW peaks during boreal summer with a maximum of 690 W m^{-2} in zone Z1 (northern Indian Ocean). Overall, FKEW in the Southern Ocean zone (Z6) is very high because of the strong westerlies that occur throughout the year. The zonal structure is well expressed, albeit a little smoother than in the summer chart; the minimum is about 100 W m^{-2} (in Z3), and the maximum is about 1500 W m^{-2} (in Z6). The PDF analysis shows that the statistical quantities estimated for the different zones are not in agreement with each other. This means that it is necessary to study the wind statistics in each zone separately. The histogram has a bimodal structure for zones Z1 and Z3 because of the influence of monsoon activity. The PDFs also confirm that the westerlies during the monsoon season are stronger in zone Z3 than in Z1. The strong winds in zone Z2 are a result of the occurrence of cyclonic activity.

Acknowledgements

The authors are grateful to Dr. S.W.A. Naqvi, Director, Council of Scientific & Industrial Research, National Institute of Oceanography (CSIR-NIO) for his constant encouragement of this collaborative work and Dr. G.S. Golitsyn, Head, Division of Atmospheric Dynamics, Institute of Atmospheric Physics of the Russian Academy of Sciences (IAP-RAS), Moscow, for fruitful discussions of the results. The buoy wind data, used for the validation of ERA-Interim winds, were provided by the Indian National Centre for Ocean Information Services, Hyderabad. Ms. R. Rashmi acknowledges CSIR for granting a Senior Research Fellowship. Soumya S. Mohan is acknowledged for the calculation of the correlation coefficients between wind speed and the climate indices.

Funding

This work was supported by a state contract from the Ministry of Education and Science of the Russian Federation [11.519.11.5023] and with the resources of CSIR-NIO, Goa, India. The NIO contribution number is [5868].

Disclosure statement

No potential conflict of interest was reported by the authors.

References

- Bauer, E. (1996). Characteristic frequency distribution of remotely sensed in situ and modeled wind speed. *International Journal of Climatology*, 16, 1087–1102. doi:10.1002/(SICI)1097-0088(199610)16:10<1087::AID-JOC68>3.0.CO;2-#
- Bhaskaran, P. K., Gupta, N., & Dash, M. K. (2014). Wind-wave climate projections for the Indian Ocean from satellite observations. *Journal of Marine Science: Research and Development*, 511, 005. doi:10.4172/2155-9910.511-005
- Cai, W., & Cowan, T. (2013). Why is the amplitude of the Indian Ocean Dipole overly large in CMIP3 and CMIP5 climate models? *Geophysical Research Letters*, 40, 1200–1205. doi:10.1002/grl.50208
- Caires, S., & Sterl, A. (2005). 100-year return value estimates for ocean wind speed and significant wave height from the ERA-40 data. *Journal of Climate*, 18(4), 1032–1048.
- Cardone, V. J., Greenwood, J. G., & Cane, M. A. (1990). On trends in historical marine wind data. *Journal of Climate*, 3, 113–127. doi:10.1175/1520-0442(1990)003<0113:OTIHMW>2.0.CO;2
- Dee, D. P., Uppala, S. M., Simmons, A. J., Berrisford, P., Poli, P., Kobayashi, S., ... Vitart, F. (2011). The ERA-Interim reanalysis: Configuration and performance of the data assimilation system. *Quarterly Journal of the Royal Meteorological Society*, 137, 553–597. doi:10.1002/qj.828
- Dong, L., Tianjun, Z., & Bo, W. (2014). Indian Ocean warming during 1958–2004 simulated by a climate system model and its mechanism. *Climate Dynamics*, 42(1–2), 203–217.
- Feng, M., & Meyers, G. (2003). Interannual variability in the tropical Indian Ocean: A two-year time-scale of Indian Ocean Dipole. *Deep Sea Research Part II: Topical Studies in Oceanography*, 50(12), 2263–2284.
- Golitsyn, G. S., Polnikov, V. G., & Pogarskii, F. A. (2012). Numerical estimates of mechanical energy transfer from the atmosphere to the Indian ocean. *Doklady Earth Sciences*, 446, Part 1, 1116–1120 (English transl).
- Gower, J. F. R. (2002). Temperature, wind and wave climatologies, and trends from marine meteorological buoys in the Northeast Pacific. *Journal of Climate*, 15, 3709–3718. doi:10.1175/1520-0442(2002)015<3709:TAWCA>2.0.CO;2
- Gulev, S. K., & Grigorieva, V. (2004). Last century changes in ocean wind waves height from global visual wave data. *Geophysical Research Letters*, 31, L24302. doi:10.1029/2004GL021040
- Han, W., Vialard, J., McPhaden, M. J., Lee, T., Masumoto, Y., Feng, M., & de Ruijter, W. P. M. (2014). Indian Ocean decadal variability: A review. *Bulletin of the American Meteorological Society*, 95, 1679–1703. doi:10.1175/BAMS-D-13-00028.1
- James, R., Holton, J. R., Curry, J. A., & Pyle, J. A. (2003). *Encyclopedia of atmospheric sciences* (Vol. 4). London: Academic Press.
- Justus, C., Hargraves, W., & Yalcin, A. (1976). Nationwide assessment of potential output from wind powered generators. *Journal of Applied Meteorology*, 15, 673–678.
- Kållberg, P., Berrisford, P., Hoskins, B., Simmons, A., Uppala, S., Lamy-Thépaut, S., & Hine, R. (2005). ERA-40 Atlas/ ERA-40 Project Report, Series No. 19. Retrieved from <https://www.awstruepower.com/assets/A-Study-of-Wind-Speed-Variability-Using-Global-Reanalysis-Data2.pdf>
- Klink, K. (2007). Atmospheric circulation effects on wind speed variability at turbine height. *Journal of Applied Meteorology and Climatology*, 46, 445–456.
- Lledó, L., Dubois, J., Barton, M. S., & Brower, M. C. (2013). A study of wind speed variability using global reanalysis data. Retrieved from <https://www.awstruepower.com/assets/A-Study-of-Wind-Speed-Variability-Using-Global-Reanalysis-Data2.pdf>
- Monahan, A. H. (2006). The probability distribution of sea surface wind speeds. Part I: Theory and sea winds observations. *Journal of Climate*, 19(2), 497–520.

- Nidheesh, A., Lengaigne, M., Vialard, J., Unnikrishnan, A., & Dayan, H. (2013). Decadal and long-term sea level variability in the tropical Indo-Pacific Ocean. *Climate Dynamics*, 41(2), 381–402.
- Phillips, O. M. (1977). *Dynamics of the upper ocean*. London: Cambridge University Press.
- Pogarskii, F. A., Polnikov, V. G., & Sannasiraj, S. A. (2012). Joint analysis of the wind and wave-field variability in the Indian Ocean for 1998–2000. *Izvestiya, Atmospheric and Oceanic Physics*, 48(6), 639–656 (in Russian: V.48, No. 6, pp 714–732).
- Polnikov, V., Pogarskii, F., & Sannasiraj, S. (2011). Statistical features of the wind field over the Indian Ocean for the period 1998–2008. Retrieved from arXiv:11095073
- Rao, S. A., Dhakate, A. R., Saha, S. K., Mahapatra, S., Chaudhari, H. S., Pokhrel, S., & Sahu, S. K. (2012). Why is Indian Ocean warming consistently? *Climatic Change*, 110(3–4), 709–719.
- Rashmi, R., Samiksha, S., Polnikov, V., Pogarskii, F., Sudheesh, K., & Vethamony, P. (2014). Spectral analysis of wind field in the Indian Ocean. *Indian Journal of Marine Sciences*, 43(7), Online Publication.
- Roxy, M. K., Ritika, K., Terray, P., & Masson, S. (2014). The curious case of Indian Ocean warming. *Journal of Climate*, 27(22), 8501–8509. doi:10.1175/JCLI-D-14-00471.1
- Saji, N. H., Goswami, B. N., Vinayachandran, P. N., & Yamagata, T. (1999). A dipole mode in the tropical Indian Ocean. *Nature*, 401, 360–363.
- Sandeep, S., & Ajayamohan, R. S. (2014). Poleward shift in Indian summer monsoon low level jetstream under global warming. *Climate Dynamics*, 45, 337–351. doi:10.1007/s00382-014-2261-y
- Sreenivas, P., Gnanaseelan, C., & Prasad, K. (2012). Influence of El Niño and Indian Ocean Dipole on sea level variability in the Bay of Bengal. *Global and Planetary Change*, 80–81, 215–225.
- Swapna, P., Krishnan, R., & Wallace, J. (2014). Indian Ocean and monsoon coupled interactions in a warming environment. *Climate Dynamics*, 42(9–10), 2439–2454.
- Thomas, B. R., Kent, E. C., Swail, V. R., & Berry, D. I. (2008). Trends in ship wind speeds adjusted for observation method and height. *International Journal of Climatology*, 28, 747–763. doi:10.1002/joc.1570
- Tokinaga, H., & Xie, S.-P. (2011). Wave- and Anemometer-Based Sea Surface Wind (WASWind) for climate change analysis. *Journal of Climate*, 24, 267–285. doi:10.1175/2010JCLI3789.1
- Uppala, S. M., Kållberg, P. W., Simmons, A. J., Andrae, U., Da Costa Bechtold, V., Fiorino, M., ... Woollen, J. (2005). The ERA-40 reanalysis. *Quarterly Journal of the Royal Meteorological Society*, 131, 2961–3012.
- Xie, S. P., Deser, C., Vecchi, G. A., Ma, J., Teng, H., & Wittenberg, A. T. (2010). Global warming pattern formation: Sea surface temperature and rainfall. *Journal of Climate*, 23, 966–986.
- Yan, Z., Bate, S., Chandler, R. E., Isham, V., & Wheeler, H. (2002). An analysis of daily maximum wind speed in northwestern Europe using generalized linear models. *Journal of Climate*, 15(15), 2073–2088.
- Young, I. R., Vinoth, J., Zieger, S., & Babanin, A. V. (2012). Investigation of trends in extreme value wave height and wind speed. *Journal of Geophysical Research*, 117, C00J06. doi:10.1029/2011JC007753
- Young, I. R., Zieger, S., & Babanin, A. (2011). Global trends in wind speed and wave height. *Science*, 332, 451–455. doi:10.1126/science.1197219
- Zheng, X. T., Xie, S. P., Du, Y., Liu, L., Huang, G., & Liu, Q. (2013). Indian Ocean Dipole response to global warming in the CMIP5 multimodel ensemble. *Journal of Climate*, 26(16), 6067–6080.
- Zieger, S., Babanin, A. V., & Young, I. R. (2014). Changes in ocean surface wind with a focus on trends in regional and monthly mean values. *Deep-Sea Research Part-I*, 86, 56–67. doi:10.1016/j.dsr.2014.01.004